

## Distribution of tunneling-level barrier heights in $(\text{KBr})_{1-x}(\text{KCN})_x$ : Comparison of dielectric response and specific heat

Richard M. Ernst, Lei Wu, and Sidney R. Nagel

*James Franck Institute and Department of Physics, The University of Chicago, Chicago, Illinois 60637*

Sherman Susman

*Materials Science Division, Argonne National Laboratory, Argonne, Illinois 60439*

(Received 23 March 1988)

We have measured the frequency-dependent dielectric response of the glassy crystal  $(\text{KBr})_{1-x}(\text{KCN})_x$  for  $x=0.25, 0.5, 0.7,$  and  $1.0$ . From the data on the pure crystal, KCN, we calculate the asymmetry energy of the two-level states which form the tunneling centers in the glassy compositions. Using the dielectric data we calculate the low-temperature specific heat and compare with experimental data. We find this calculated specific heat to have the same magnitude, composition dependence, and time dependence as seen in those experiments. This gives strong support to a microscopic theory of the glassy dynamics of this system. We also find the data to be consistent with a mean-field theory of the quadrupolar ordering transition in  $(\text{KBr})_{1-x}(\text{KCN})_x$ . We relate the number of low-temperature tunneling levels to the quadrupolar transition temperature. The relevance of this microscopic model for understanding the glassy behavior in real structural glasses is discussed.

### I. INTRODUCTION

The mixed ionic crystal  $(\text{KBr})_{1-x}(\text{KCN})_x$  presents an ideal system in which to explore the glassy state. Numerous measurements by a variety of techniques have indicated that this material has all of the traditional experimental features of a glass. What makes  $(\text{KBr})_{1-x}(\text{KCN})_x$  particularly deserving of our attention, though, is that this "glass" is actually a crystal with a well-characterized structure, making it possible to calculate the properties of this glassy system from first principles.

That  $(\text{KBr})_{1-x}(\text{KCN})_x$  is a glasslike crystal is well established. The system shows a low-temperature specific heat which is time dependent and approximately linear in temperature.<sup>1,2</sup> This crystal has a thermal conductivity proportional to  $T^2$ , with a magnitude comparable to what one measures in real glasses.<sup>1,2</sup> Several experimental probes, including inelastic neutron scattering,<sup>3-5</sup> Brillouin scattering,<sup>6</sup> x-ray diffraction,<sup>7</sup> and ultrasonic,<sup>3,8</sup> dielectric,<sup>3,9</sup> and shear-response<sup>10</sup> studies, indicate a relaxational transition at high temperature in which  $(\text{KBr})_{1-x}(\text{KCN})_x$  freezes into an orientationally disordered state. This transition is reminiscent of a real glass transition in supercooled liquids.  $(\text{KBr})_{1-x}(\text{KCN})_x$  also has an anomalously broad dielectric<sup>11,12</sup> and mechanical response,<sup>10</sup> which is analogous to the  $\beta$  relaxation found in glasses in the intermediate-temperature regime.<sup>13</sup> The dielectric  $\beta$  relaxation is the focus of the present study. We will show that from  $\beta$ -relaxation measurements one gains a great deal of information about not only the dynamics at the measurement temperature, but about low-temperature thermal properties and the high-temperature "glass" transition as well.

Ordinary glasses are difficult to deal with theoretically owing to our ignorance of their microscopic local structure. The very successful two-level system model of Anderson, Halperin, and Varma,<sup>14</sup> and Phillips<sup>15</sup> makes a good deal of progress toward a phenomenological understanding of the low-temperature behavior of glasses. In this model, one hypothesizes the existence of some two-level tunneling centers with a distribution of asymmetry and barrier energies. If these tunneling centers dominate the low-temperature dynamics of the glass, then one can produce a specific heat linear in temperature and a thermal conductivity proportional to  $T^2$  by choosing appropriate distributions of energies. We have little feeling, however, for the microscopic nature of these tunneling centers and for their actual distribution. In  $(\text{KBr})_{1-x}(\text{KCN})_x$ , on the other hand, we believe that we have a microscopic picture for the dynamics. The cyanide molecules have two possible orientations separated by a  $180^\circ$  flip. Tunneling (at low temperature) and thermal activation (at intermediate temperature) between the two orientations are the dynamical processes which lead, respectively, to the low-temperature specific heat and intermediate-temperature dielectric response. A recent theory by Sethna *et al.*<sup>16</sup> takes this picture of flipping dipoles and ties together the low-temperature thermal properties of  $(\text{KBr})_{1-x}(\text{KCN})_x$  and the intermediate-temperature  $\beta$  relaxation. A mean-field theory<sup>17</sup> relates the dielectric response to the high-temperature glasslike transition.

In this paper we present our data from a systematic study of the frequency-dependent dielectric response of  $(\text{KBr})_{1-x}(\text{KCN})_x$  as a function of CN concentration:  $x=0.25, 0.5, 0.7,$  and  $1.0$ . Measurements on pure KCN give us information on the asymmetry energy of the two-

level system. This will allow us to compare the calculations of Sethna's model with the experiments in absolute units. The other three compositions span the range in  $x$  over which glassy low-temperature thermal properties are observed. For all three glassy samples, we see very broad log-normal dielectric dissipation peaks at all temperatures, which we conclude arise from Gaussian distributions of activation energies. We calculate the density of tunneling states, and find agreement with the composition dependence measured by low-temperature specific-heat studies to within 6%. The linear specific heat we calculate agrees with experiment in both composition dependence and time dependence to a remarkable degree. We also observe a weak temperature dependence in the distribution of tunneling states, which is consistent with the mean-field theory.

This paper is organized as follows. In Sec. II we review the  $(\text{KBr})_{1-x}(\text{KCN})_x$  system, as well as the microscopic model used in the theories. In Sec. III we describe the experimental technique used to measure the dielectric response over a broad frequency range. Section IV contains our experimental results along with a detailed discussion of the data analysis. In Sec. V we compare our results with theory and other experiments. We show that our measurements are consistent with the microscopic model of  $(\text{KBr})_{1-x}(\text{KCN})_x$ , and we speculate as to how our findings extrapolate to the larger problem of the glassy state in general.

## II. BACKGROUND

### A. The $(\text{KBr})_{1-x}(\text{KCN})_x$ system

$(\text{KBr})_{1-x}(\text{KCN})_x$  is an ionic crystal with a NaCl lattice structure.<sup>12</sup> CN molecules replace Br ions at random lattice sites. The CN molecules are dumbbell-shaped objects possessing a small electric dipole moment ( $p \sim 0.07 e \text{ \AA}$ ). Since CN and Br are of roughly equal sizes, replacement of one by the other does not appreciably distort the lattice, and it is possible to vary the CN concentration over the entire range  $0 \leq x \leq 1$ . The system thus has tunable disorder as evidenced by the phase diagram of  $(\text{KBr})_{1-x}(\text{KCN})_x$ .<sup>7</sup> At very small values of  $x$  one sees independent CN dipole oscillators, at  $x \approx 1$  one sees long-range order in CN orientation, and at intermediate values one sees a disordered, orientational glass.

For  $0.2 < x < 0.57$ ,  $(\text{KBr})_{1-x}(\text{KCN})_x$  is characterized as an orientational glass.<sup>3,4,8,12</sup> At high temperature, the CN molecules are free to rotate in place. Below a composition-dependent transition temperature  $T_q$ , quadrupolar strain fields dominate the motion, and the quadrupolar axes freeze into random orientations. In this glassy state the CN dipoles, however, are still free to flip by  $180^\circ$ , with a reorientation barrier separating the two stable dipole configurations. The energy barrier is caused by quadrupolar strain fields, the product of the local random CN environment. There is a small asymmetry energy between the two dipole orientations, caused by the unequal sizes of the C and N atoms, and by electric dipole interactions.

Above  $x = 0.57$  the CN quadrupoles freeze into a state with long-range order. At the  $x = 1.0$  extreme of this composition range, one observes two phase transitions.<sup>12</sup> Pure KCN undergoes a ferroelastic transition at 168 K, at which point the crystal becomes orthorhombic, and the quadrupoles all line up along a single  $\langle 110 \rangle$  direction. The dipoles retain the freedom to flip by  $180^\circ$  in this phase. Below 83 K, the dipoles order antiferroelectrically, with alternating (001) planes having opposing dipole orientations. For  $x \lesssim 0.75$ , the system does not order antiferroelectrically, and glassy properties are observed. Enough quadrupolar orientational and substitutional disorder exists at these concentrations, even though long-range order is present, to result in glassy behavior.

### B. Tunneling-level theories of $(\text{KBr})_{1-x}(\text{KCN})_x$

The theory due to Sethna *et al.*<sup>16</sup> of the glassy dynamics of  $(\text{KBr})_{1-x}(\text{KCN})_x$  assumes that dipole flipping is the dominant dynamical process responsible for all of the observed glassy behavior. The two stable dipole orientations are identified as the potential wells of the two-level system.  $\beta$  relaxation measured in dielectric-response studies indicates a broad distribution of activation energies.<sup>11,18</sup> This distribution of barrier heights,  $P(E)$ , forms the starting point for the analysis.

At high temperature, thermal activation over the barriers is the principal relaxational mode, so that a wide range of energy barriers is probed by high-temperature dielectric studies. At low temperatures, tunneling through the barrier dominates, so that one is sensitive only to dipoles which can tunnel within the duration of a low-temperature measurement. The rate of CN tunneling between the two stable orientations is

$$\Gamma(E) = \Gamma_0 \exp(-4\sqrt{2IE}/h), \quad (1)$$

where  $\Gamma_0$  is the attempt frequency of  $8.3 \times 10^{13}$  Hz, and  $I$  is the effective CN moment of inertia,  $2.65 \times 10^{-39}$  g cm<sup>2</sup>. The probability that a CN molecule with barrier energy  $E$  can tunnel within a time  $t$  is then  $\{1 - \exp[-\Gamma(E)t]\}$ . The density of tunneling states per unit volume per unit energy that can tunnel within time  $t$  is

$$\mathcal{P}(x, t) = n(\delta) \frac{x}{A} \int_0^\infty dE P(E) \{1 - \exp[-\Gamma(E)t]\}, \quad (2)$$

where  $x$  is the CN concentration,  $A$  is the volume per unit cell, and  $P(E)$  is the distribution of barrier energies.  $n(\delta)$  is the fraction of tunneling centers per unit energy with energy splitting  $\delta$ . Sethna has made the traditional two-level-system assumption that  $n(\delta)$  is a constant:  $n(\delta) = n_0 = 1/\Delta_0$ . Here  $\Delta_0$  is the zero-temperature asymmetry energy for pure KCN. The energy-splitting distribution is thus taken to be constant over the energy scale given by  $\Delta_0$ , and is uncorrelated with  $E$ . It is further assumed that  $n(\delta)$  is independent of CN concentration. The low-temperature specific-heat  $C_p$  is proportional to  $\mathcal{P}(x, t)$ , so that a constant  $n(\delta)$  leads directly to a  $C_p$  linear in  $T$ . Sethna *et al.*<sup>16</sup> have applied this model to  $(\text{KBr})_{0.5}(\text{KCN})_{0.5}$  with satisfactory results. There is only one free parameter in the calculation,  $n_0$ . They find that choosing  $n_0 = 1/(314 \text{ K} k_B)$  gives a value for  $C_p(t)$  in

agreement with low-temperature specific-heat measurements. We can make a more precise test of this model by studying the composition dependence of  $\mathcal{P}(x, t)$  and comparing it to experimental results for the specific heat.

The rate expression in curly braces in Eq. (2) is approximately a step function, with a value  $\approx 0$  for  $E > E_{\max}$ .  $E_{\max}$  is the barrier energy which yields a tunneling rate  $\Gamma(E_{\max})=1/t$ ; for  $t=1$  sec,  $E_{\max}/k_B=96$  K. This means that accurate determination of  $P(E)$  in the low-energy tail is crucial for this analysis.

A related mean-field theory (Ref. 17) applies the same microscopic model of  $(\text{KBr})_{1-x}(\text{KCN})_x$  to the quadrupolar freezing transition. The transition is characterized by a quadrupolar order parameter (i.e., the net alignment of the CN quadrupoles) which this theory indicates should decrease linearly with increasing  $T$  at low temperature. The dynamics of the dipoles probes this order parameter of the quadrupoles in  $(\text{KBr})_{1-x}(\text{KCN})_x$  since the energy barriers to dipole reorientation are created by the quadrupolar order. Therefore, since the energy barriers and the transition temperature are both proportional to the strength of the quadrupolar interaction, they should be proportional to one another.

### III. EXPERIMENTAL TECHNIQUE

We measured the complex dielectric constant  $\epsilon = \epsilon' + i\epsilon''$  of  $(\text{KBr})_{1-x}(\text{KCN})_x$  by placing the samples between two capacitor plates. We used samples which were square single-crystal slabs, about 1 cm on a side and 1 mm thick. Because cyanide is hygroscopic and, of course, highly toxic, all sample preparation was done in a dry nitrogen atmosphere using a glove box. Capacitor plates made of aluminized Mylar or copper foil and Mylar were attached with VacSeal oil to the samples, with the insulator side in, in order to prevent the interaction of the metal with the cyanide. We soldered or silver epoxied two coaxial cables to each capacitor plate, allowing for four-probe measurements. To stabilize the temperature, the samples were held between two electrically insulated copper disks 3 cm in diameter and 5 mm thick, with only gentle pressure applied so as not to crack the fragile crystals. We measured the temperature with Au-Fe thermocouples placed near the capacitor, one on each copper disk to detect any thermal gradients across the sample.

A heater made of Nichrome wire surrounded the copper disks. The entire assembly was mounted in an evacuated copper can, which was cooled in a  $^4\text{He}$  Dewar. A Hewlett-Packard desktop computer controlled the temperature, to an accuracy of  $\pm 0.1$  K, and logged all data as well.

For measurements between 10 kHz and 10 MHz, we used a Hewlett-Packard 4275 A multifrequency LCR meter, which measures the capacitance and dielectric-loss factor, proportional to  $\epsilon'$  and  $\epsilon''/\epsilon'$ , respectively. Between 0.2 Hz and 10 kHz we employed a lock-in technique to measure  $\epsilon$ . A sinusoidal voltage was applied across the capacitor with a Hewlett-Packard 3326A frequency synthesizer. A Keithley 427 current amplifier produced a voltage proportional to the current through the sample. A PAR 124A or PAR 5301 lock-in amplifier (PAR denotes Princeton Applied Research) served as the phase-sensitive detector, with the in-phase and out-of-phase signals proportional to  $\epsilon''$  and  $\epsilon'$ , respectively. The phase was accurately zeroed by substituting an air capacitor for the sample capacitor. Below 0.2 Hz we used a homemade digital lock-in amplifier (described in detail elsewhere<sup>19</sup>) in place of the commercial units mentioned above. Using a Keithley 193 voltmeter and 705 scanner, we digitally sampled the output of the current amplifier along with the output of the synthesizer, which served as the phase reference. Fourier decomposition of the sampled waveform yields the in-phase and out-of-phase components of the current, and thus  $\epsilon''$  and  $\epsilon'$ .

$\epsilon'$  is larger than  $\epsilon''$  typically by a factor of  $10^3$ , so that good phase stability in the lock-in measurement is essential. The total signal is proportional to the measuring frequency  $\omega$ , and above 1 Hz phase stability is quite good. Below 1 Hz, however, it becomes necessary to use considerably longer measurement times in order to achieve good accuracy, as much as 30 min per measurement at the lowest frequency (0.03 Hz). To probe lower in frequency than our limit of 0.03 Hz using this technique is not practical. Typical errors in  $\epsilon''$  range from less than 1% at high frequency to about 5% at low frequency.

We took data by ramping temperature at fixed frequency from the base temperature, about 4.5 K, to about 70 K, with measurements taken approximately every 1 K. We normalized the raw data to have the same value for  $\epsilon'$  at high temperature for all frequencies. Representative plots of temperature-domain data are found in Fig. 1. By

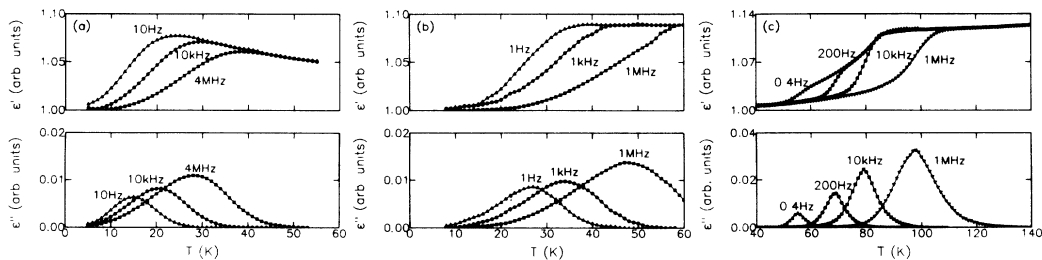


FIG. 1. Temperature-domain dielectric data for  $(\text{KBr})_{1-x}(\text{KCN})_x$ . Graphs show  $\epsilon'$  and  $\epsilon''$  vs  $T$  for (a)  $x=0.25$ , (b)  $x=0.7$ , and (c)  $x=1.0$ . The vertical axes in the three graphs are scaled to different arbitrary units, where  $\epsilon'$  and  $\epsilon''$  for a given concentration are given in the same units.

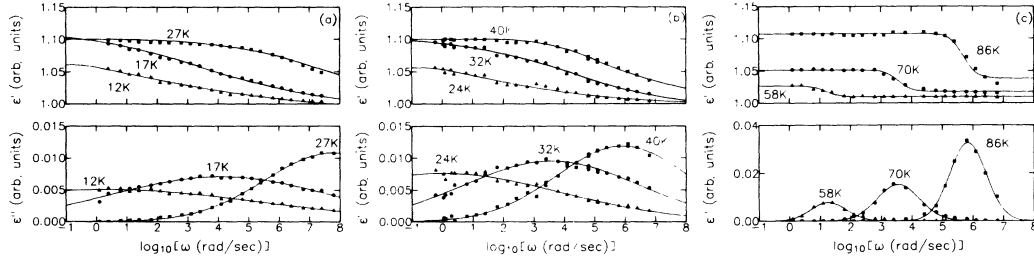


FIG. 2. Frequency-domain data, showing  $\epsilon'$  and  $\epsilon''$  vs  $\log_{10}(\omega)$  for (a)  $x=0.25$ , (b)  $x=0.7$ , and (c)  $x=1.0$ . The smooth curves indicate least-squares fits to a convolution [Eq. (12)] of a Gaussian distribution of activation energies with a Debye response for each energy.

making constant-temperature cuts through the temperature-domain data, we obtain the frequency-domain curves represented in Fig. 2. Note that all curves show symmetric response, moving toward higher peak frequencies and narrower widths with increasing temperature. The glassy compositions have very broad dielectric response. We remark here that we will ultimately want information on the high-frequency side of the response curves for comparison with low-temperature specific-heat measurements. Although measuring at low temperatures will shift this part of the curve into our experimental frequency range, such a procedure is not satisfactory. This is because the  $\epsilon''(\omega)$  curves become infinitely broad at zero temperature so that frequency, and not temperature, is the limiting experimental parameter in our experiment.

#### IV. RESULTS

##### A. Pure KCN

We have measured the dielectric response of KCN in the vicinity of the antiferroelectric phase transition and are able to derive from the data a value for the asymmetry energy between the two CN dipole orientations. The plots of  $\epsilon''$  versus  $\log_{10}(\omega)$  in Fig. 2(c) indicate an approximately Debye dissipation peak at temperatures above the transition at 83 K:

$$\epsilon(\omega) = \epsilon_{\infty} + (\epsilon_0 - \epsilon_{\infty}) \frac{1}{1 + i\omega\tau}. \quad (3)$$

Here,  $\epsilon_0$  and  $\epsilon_{\infty}$  are, respectively, the low- and high-frequency values for  $\epsilon(\omega)$ . The peaks broaden at lower temperatures in the antiferroelectric phase. Although broader than a Debye peak, these peaks are still sufficiently narrow that they can be fitted equally well by a number of standard functional forms, including Cole-Cole:<sup>20</sup>

$$\epsilon(\omega) = \epsilon_{\infty} + (\epsilon_0 - \epsilon_{\infty}) \frac{1}{1 + (i\omega\tau)^{1-\alpha}}, \quad (4)$$

Kohlrausch-Williams-Watts (or stretched exponential):<sup>21</sup>

$$\epsilon(\omega) = \epsilon_{\infty} + (\epsilon_0 - \epsilon_{\infty}) \mathcal{F} \left\{ \frac{d}{dt} \exp[-(t/\tau)^{\beta}] \right\} \quad (5)$$

(where  $\mathcal{F}\{\dots\}$  denotes the complex Fourier transform), and log-normal:

$$\epsilon''(\omega) = (\epsilon_0 - \epsilon_{\infty}) \frac{1}{\sqrt{\pi W}} \times \exp[-(\log_{10}\omega - \log_{10}\omega_p)^2 / W^2]. \quad (6)$$

The Debye form is characteristic of systems with a single barrier energy. The Cole-Cole and Kohlrausch-Williams-Watts curves are empirical forms used to fit broader distributions.

The behavior of the static dielectric susceptibility,<sup>22</sup>  $\chi \equiv \epsilon_0 - \epsilon_{\infty}$ , gives us an indication of the phase transition at 83 K. We can obtain values for  $\chi$  from either  $\epsilon'$  or  $\epsilon''$ . In the present study we have used  $\epsilon''$  at low temperatures:

$$\epsilon_0 - \epsilon_{\infty} = \int_0^{\infty} d\omega \frac{\epsilon''(\omega)}{\omega}. \quad (7)$$

At high temperature, we obtain  $\chi$  by measuring  $\epsilon_0$  and  $\epsilon_{\infty}$  separately. To do this we use the temperature-domain graphs (Fig. 1) and extrapolate  $\epsilon_{\infty}$  linearly to high temperatures. Figure 3 shows  $1/\chi$  versus  $T$ ; notice the cusp at the transition temperature. The standard mean-field-theory description of an antiferroelectric phase transition holds that

$$1/\chi = T \operatorname{sech}^2[\Delta(T)/2T] + \Theta, \quad (8)$$

where  $\Delta(T)$  is the asymmetry energy and  $\Theta$  is the Curie-Weiss temperature. We can solve for  $\Delta(T)$  using the self-consistent mean-field relation

$$\Delta(T) = \Delta_0 \tanh[\Delta(T)/2T].$$

This form fits the data quite well, as the smooth curve in Fig. 3 indicates. The least-squares value for  $\Delta_0/k_B$  is 260 K. Alternatively, we can determine  $\Delta_0$  by using the relation

$$\Delta(T) = \Delta_0 (1 - T/T_c)^{1/2},$$

which is the proper form for an Ising antiferromagnet. This second form yields  $\Delta_0/k_B = 340$  K. We can use these values to get a rough estimate of the asymmetry energy at zero temperature:  $\Delta_0/k_B \approx 300 \pm 40$  K. This value is consistent with the choice  $n_0^{-1}/k_B = \Delta_0/k_B = 314$

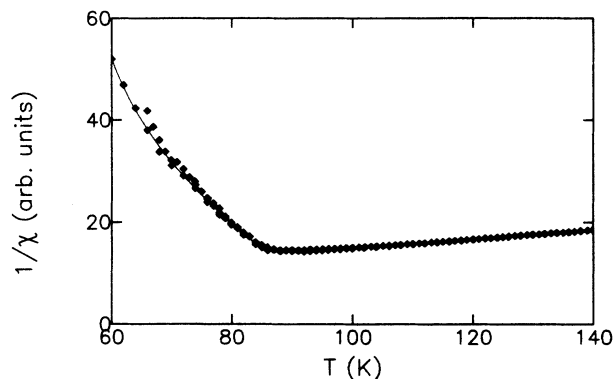


FIG. 3. Inverse dielectric susceptibility  $1/\chi$  of KCN vs temperature. Note the cusp at 83 K, indicating an antiferroelectric transition. The smooth curve indicates the best fit to Eq. (8), with  $\Theta = 55 \pm 10$  K.

K used by Sethna to fit the time-dependent specific heat of  $(\text{KBr})_{0.5}(\text{KCN})_{0.5}$ .

### B. Mixed crystals

We have similarly measured the very broad dielectric response of the three glassy compositions,  $x = 0.25, 0.5$  (see Ref. 11), and 0.7, all below their quadrupolar transition temperatures. We fit the imaginary frequency-domain data,  $\epsilon''(\omega, T)$  to five functional forms: Kohlrausch-Williams-Watts, Davidson-Cole,<sup>23</sup> log-normal, Cole-Cole, and a form based on a binomial distribution of barrier heights. The log-normal (or possibly Cole-Cole) fits give consistently the best results as was previously found for the  $x = 0.5$  composition.<sup>11</sup> We treat each cyanide concentration  $x$  as a separate data set and look for trends in the fit parameters as a function of temperature.

The Kohlrausch-Williams-Watts form [Eq. (5)] tends to be too asymmetrical and shows adequate agreement with the data for only a few temperatures. The Davison-Cole form,

$$\epsilon(\omega) = \epsilon_{\infty} + (\epsilon_0 - \epsilon_{\infty}) \frac{1}{(1 + i\omega\tau)^{\alpha}}, \quad (9)$$

is another empirical generalization of Debye often seen in amorphous systems. This is the most asymmetrical of the forms we have tried, and not surprisingly performs quite poorly on our data, which is symmetrical.

Log-normal fits [Eq. (6)] to the dielectric data are consistently the best throughout the entire range of composition and temperature. From the fits, we obtain the peak frequency,  $\omega_p$ , and the  $1/e$  half-width of the peak,  $W$ . We plot these fit parameters in Fig. 4. The last remaining fitting function is Cole-Cole [Eq. (4)]. This form is nearly indistinguishable from log-normal, and therefore is no better at fitting our data. We find it preferable to continue with the log-normal fits, though, since these will lead immediately to a reasonable form for the distribution of activation energies, as we show below.

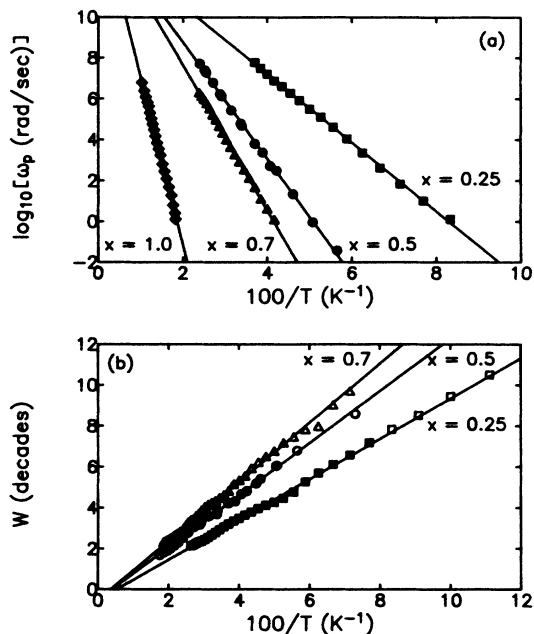


FIG. 4. (a) Plot of  $\log_{10}(\omega_p)$  vs  $100/T$  for all four compositions. The straight lines indicate activated behavior. Best-fit parameters ( $E_0$  and  $\omega_0$ ) are given in Table I and Fig. 5. (b) Width of the  $\epsilon''(\log_{10}\omega)$  peaks,  $W$  vs  $100/T$  for the three glassy compositions. The data are fitted to a straight line. Solid symbols indicate temperatures for which  $\omega_p$  falls within our measurement range, and for which a three-parameter log-normal fit was used. Open symbols are for those temperatures where  $\omega_p$  is outside this range, and where  $\omega_p$  was fixed by extrapolation of the Arrhenius plot. Data for  $x = 0.5$  are from Ref. 11.

Arrhenius plots of  $\log_{10}(\omega_p)$  versus  $100/T$  for all four compositions are shown in Fig. 4(a). All four cases show an activated form:

$$\omega_p = \omega_0 e^{-E_0/k_B T}. \quad (10)$$

The activation energies  $E_0$  and effective attempt frequencies  $\omega_0$  of these fits are summarized in Table I and Fig. 5.

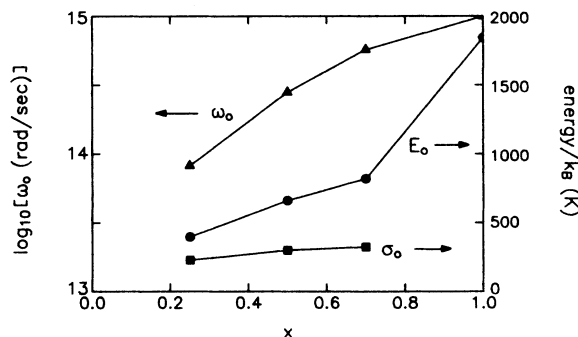


FIG. 5. Summary of fit parameters, showing the peak energy ( $E_0$ ), distribution width ( $\sigma_0$ ), and measured attempt frequency ( $\omega_0$ ) as a function of CN concentration  $x$ . Data for  $x = 0.5$  are from Ref. 11.

TABLE I. Energy scale and density-of-states data for  $(\text{KBr})_{1-x}(\text{KCN})_x$ .  $\omega_0$  is the measured attempt frequency.  $E_0$  is the average activation energy at zero temperature.  $\sigma_0$  is the width of the barrier height distribution, extrapolated to zero temperature using  $\sigma = Wk_B T \ln(10)$ .  $T_q$  is the quadrupolar freezing temperature, taken from Ref. 6.  $\beta$  and  $\alpha$  are the slopes of  $\sigma_0$  and  $E_0$  vs  $T$ , respectively.  $\mathcal{P}(x, t = 1 \text{ sec})/\mathcal{P}(x = 0.7, t = 1 \text{ sec})$  is the normalized density of tunneling states for  $t = 1$  sec. Values are taken from the present study ( $\epsilon$ ) and from the specific-heat measurements ( $C_p$ ) of De Yoreo *et al.* (Ref. 1). Dielectric data for  $x = 0.5$  are from Ref. 11.

$x$	0.25	0.5	0.7	1.0
$\omega_0$ (rad/sec)	$(8.2 \pm 2) \times 10^{13}$	$(2.8 \pm 1) \times 10^{14}$	$(5.7 \pm 1) \times 10^{14}$	$(9.9 \pm 2) \times 10^{14}$
$E_0/k_B$ (K)	$397 \pm 7$	$660 \pm 7$	$820 \pm 7$	$1842 \pm 10$
$\sigma_0/k_B$ (K)	$228 \pm 10$	$300 \pm 10$	$324 \pm 10$	
$\sigma_0/E_0$	$0.574 \pm 0.02$	$0.455 \pm 0.02$	$0.395 \pm 0.02$	
$T_q$ (K)	$49 \pm 2$	$80 \pm 2$	$103 \pm 3$	$168 \pm 3$
$E_0/k_B T_q$	$8.1 \pm 0.9$	$8.3 \pm 0.5$	$8.0 \pm 0.3$	$11.0 \pm 0.2$
$\beta/k_B$	$1.15 \pm 0.1$	$1.42 \pm 0.1$	$1.35 \pm 0.1$	
$\alpha/k_B$	$2.00 \pm 0.2$	$3.13 \pm 0.2$	$3.42 \pm 0.2$	
$\frac{\mathcal{P}(x, 1 \text{ sec})}{\mathcal{P}(x = 0.7, 1 \text{ sec})} \{\epsilon\}$	$14.0 \pm 2.3$	$3.4 \pm 0.8$	$1.0 \pm 0.4$	
$\frac{\mathcal{P}(x, 1 \text{ sec})}{\mathcal{P}(x = 0.7, 1 \text{ sec})} \{C_p\}$	$14.8 \pm 1.5$	$3.3 \pm 0.4$	$1.0 \pm 0.1$	

In order to find the best log-normal fits to our data, we use a three-parameter fit for these temperatures, where  $\omega_p$  is within our measurement range. Outside that range we use a two-parameter fit with  $\omega_p$  determined by Eq. (12). The best-fit values for  $W$  obtained in this manner are plotted in Fig. 4(b).

We can now extract from our data the distribution of activation energies for the density-of-states calculation. We can express the dielectric response  $\epsilon(\omega, T)$  as a convolution of the distribution of relaxation times  $P(\tau)$ , with a Debye curve for each value of  $\tau$ :

$$\epsilon(\omega, T) = \epsilon_\infty + (\epsilon_0 - \epsilon_\infty) \int_0^\infty d\tau P(\tau) \frac{1}{1 - i\omega\tau}. \quad (11)$$

Such a convolution implies implicitly that the dynamics of the system can be reduced to a superposition of independent one-body motions, which need not always be the case. If we replace  $\tau$  in Eq. (11) by  $1/\omega_p$  in Eq. (10), we have a choice as to whether  $P(\tau)$  is due to a distribution of barrier energies  $E$  or to a distribution of attempt frequencies  $\omega_0$ . Since the observed dielectric response is so broad in the glassy systems, it is more reasonable to assume a distribution of energies rather than a distribution of  $\omega_0$  which would have to span many orders of magnitude to account for the observed behavior. The picture of flipping dipoles also makes it plausible that the reorientations are independent of one another, considering that a flipped dipole does little to affect the quadrupolar strain fields which determine the barriers for its neighbors. The distribution of barrier heights would come from a variation in the environment of the separate CN molecules. The dielectric response can now be written as

$$\epsilon(\omega, T) = \epsilon_\infty + (\epsilon_0 - \epsilon_\infty) \int_0^\infty dE P(E) \times \frac{1}{1 - i(\omega/\omega_0)e^{E/k_B T}}, \quad (12)$$

where the expression is the convolution of the distribution of activation energies,  $P(E)$ , with a Debye curve for each energy.

Because a wide dielectric response  $\epsilon''(\omega)$  implies an energy distribution  $P(E)$  much wider than  $k_B T$ , we can approximate the Debye response in Eq. (12) by a Dirac  $\delta$  function:

$$\text{Im} \left[ \frac{1}{1 - i(\omega/\omega_0)e^{E/k_B T}} \right] \approx \delta(\omega/\omega_0 - e^{-E/k_B T}). \quad (13)$$

There is little loss of accuracy in making this approximation, considering that  $\epsilon''(\log_{10}\omega)$  is typically 10 decades wide full width at half maximum (FWHM) as opposed to the 1.1 decades FWHM for a simple Debye curve. Equation (13) simplifies calculations, particularly fitting routines. For completeness, all results presented in this article were verified using the full integral expression for  $\epsilon''$  [Eq. (12)]; where there is a difference in results between the approximation [Eq. (13)] and the full calculation, we have so indicated. It is clear that using the approximation of Eq. (13) in Eq. (12) results in

$$\epsilon''(\omega, T) = (\epsilon_0 - \epsilon_\infty) P[E = -k_B T \ln(\omega/\omega_0)]. \quad (14)$$

Thus a Gaussian distribution of energy barriers leads to a log-normal dielectric-response curve. The log-normal form is therefore intuitively appealing since a sta-

tistical distribution of local CN environments might lead naturally to a Gaussian distribution of barrier energies. The final two fitting forms we have mentioned were log-normal and Cole-Cole. Although they both fit our data equally well, the former leads to a Gaussian distribution of energy barriers which has a simple physical interpretation. It is not clear what analysis could be done in a similar vein using the Cole-Cole fits.

Since it is clear that the dielectric response can be derived from a distribution of barrier heights, we have also tried to fit our data using a binomial distribution for  $P(E)$ . A binomial distribution results from an equal contribution to the barrier energy by each CN nearest neighbor. Since the CN molecules are randomly distributed in space, there is a probability  $x$  that a given neighbor is a CN and not a Br. We assume that each CN nearest neighbor contributes an energy  $J$  to the barrier, and that the distribution is a smooth function of energy:

$$P(E) = \frac{\Gamma(n_{\max} + 1)}{\Gamma(E/J + 1)\Gamma(n_{\max} - E/J + 1)} \times x^{E/J}(1-x)^{(n_{\max} - E/J)} \quad (15)$$

$\Gamma$  is the gamma function and  $n_{\max}$  is the total number of nearest neighbors, which for a fcc lattice is 12. We obtain  $\epsilon''(\omega, T)$  through Eq. (14). The least-squares fits we obtain are fair, but are slightly too asymmetrical for our data.

Returning to the log-normal fits to  $\epsilon''(\log_{10}\omega)$  (which were the only ones that consistently fit our data well and led to a simple analysis in terms of a distribution of barrier heights), we now find the parameters of the Gaussian distribution of energy barriers:

$$P(E) = \frac{1}{\sqrt{\pi}\sigma} \exp[-(E - E_0)^2/\sigma^2] \quad (16)$$

with peak energy  $E_0$  and width  $\sigma$ . We normalize the integrated probability to unity, ignoring the very small tail for  $E < 0$ .  $E_0$  is the average activation energy, listed in Table I, which we obtained from our Arrhenius fits. Substituting Eq. (16) into Eq. (12) gives us the fitting form for our dielectric response:

$$\epsilon(\omega, T) = \epsilon_{\infty} + (\epsilon_0 - \epsilon_{\infty}) \int_0^{\infty} dE \frac{1}{\sqrt{\pi}\sigma} \times \exp[-(E - E_0)^2/\sigma^2] \times \frac{1}{1 - i(\omega/\omega_0)e^{E/k_B T}} \quad (17)$$

Taking the  $\delta$ -function approximation for the Debye response outlined above, we calculate  $\sigma$  by

$$\sigma = Wk_B T \ln(10) \quad (18)$$

In Fig. 4(b) we see that  $W = a(1/T) - b$  with  $a$  and  $b$  positive constants.  $\sigma(T)$  is then also linear,

$$\sigma = \sigma_0 - \beta T \quad (19)$$

$\sigma_0$  is the zero-temperature width of the energy-barrier distribution, which we obtain by assuming a linear extra-

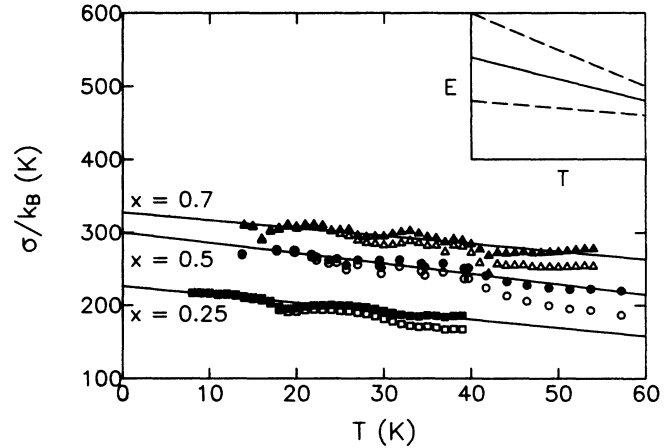


FIG. 6. Width of the energy-barrier distribution  $\sigma$  vs  $T$  for three compositions. Solid symbols indicate values calculated using  $\sigma = Wk_B T \ln 10$ , which are extrapolated linearly to zero temperature. Open symbols indicated  $\sigma$  values calculated using the full, integral form for the dielectric response [Eq. (12)]. Note that the solid and open symbols converge at low temperature. Data for  $x = 0.5$  are from Ref. 11. Inset: Schematic representation of the barrier-height distribution as a function of temperature. The solid line indicates the average barrier height, and the vertical distance between the dashed lines indicates the distribution width.

polation to  $T = 0$ . The  $\delta$ -function approximation we used is asymptotically correct at zero temperature, where the dielectric response becomes infinitely broad, so this extrapolation is justified.

Alternatively, we find  $\sigma(T)$  by using the full, integral form of the convolution; we solve iteratively for  $\sigma(T)$ .  $\sigma$  values calculated in this second way are consistently smaller than the values from the  $\delta$ -function approach, with the gap between them widening with increasing temperature. This is due to the finite width of the Debye curve. To extrapolate these values to zero temperature (and thus arrive at an alternate value for  $\sigma_0$ ), we use a properly scaled curve of the quadrupolar order parameter from the phase-transition model.<sup>17</sup> We have assumed that  $\sigma$  is proportional to the order parameter. The two values for  $\sigma_0$  thus calculated agree with one another to within the error in fitting the extrapolated curves. For comparison,  $\sigma(T)$  values calculated by both methods are plotted in Fig. 6.

We have fitted the real part of Eq. (12) to  $\epsilon'(\omega)$ , using a Gaussian distribution of energy barriers with the same fit parameters obtained from the fits to  $\epsilon''(\omega)$ . Least-squares fits to  $\epsilon'$  and  $\epsilon''$  appear in Fig. 2. The quality of the fits indicates that our data satisfy the Kramers-Kronig relations, since Eq. (12) is constrained to do so by the Debye-response curve it contains.

## V. DISCUSSION

### A. Absolute magnitude of $C_p$

We now compare calculations based on our dielectric study with the low-temperature specific-heat measure-

ments of De Yoreo *et al.*<sup>1</sup> The magnitude in absolute units of the value calculated from the Sethna model<sup>16</sup> shows surprisingly good agreement with experiment, considering the approximations involved. Recall that the specific heat is proportional to the density of tunneling states which can tunnel within the time duration of the measurement. This density-of-states calculation is based on the implicit assumption that the asymmetry and barrier energies of the two-level tunneling system are uncorrelated, as in the tunneling-level model. This standard approximation is plausible in  $(\text{KBr})_{1-x}(\text{KCN})_x$ , since we know that the asymmetry energy depends on dipolar, while the barrier height depends on quadrupolar, interactions. To obtain the total density of tunneling states, one then integrates the distribution of asymmetries and barriers over all energies. The integration over barrier energies is cut off at some upper limit, since a CN molecule will be unable to tunnel within the duration of the specific-heat measurement if the barrier is too high. The integration over asymmetry energies is simplified by the assumption that the density of asymmetries is flat on the scale of  $k_B T$ ; this step leads directly to the linear  $T$  dependence of  $C_p$  calculated by the two-level-system model. Sethna *et al.* thus take the density of asymmetry energies,  $n(\delta)$ , to be constant over an energy scale given by the maximum asymmetry energy,  $\Delta_0$ . They use this number,  $n(\delta) = n_0 = 1/\Delta_0$ , as a free parameter in their comparison of the calculated  $C_p$  with experiment for the  $x = 0.5$  composition. The value of  $n_0^{-1}/k_B$  thus obtained is 314 K.

Our measurements of the asymmetry energy of pure KCN yield a value in agreement with the number that Sethna *et al.* assume in their calculations. The  $\Delta_0/k_B = 300 \pm 40$  K we find brackets  $n_0^{-1}$ , thus lending credibility to the general approach used in the model. That the fit parameter  $n_0^{-1}$  is within experimental error of our measured  $\Delta_0$  is perhaps fortuitous; we should not have expected such good agreement, since  $\Delta_0$  pertains to the pure KCN system, while  $n_0^{-1}$  fits calculations to  $(\text{KBr})_{0.5}(\text{KCN})_{0.5}$ . Moreover, we have no guarantee that  $n(\delta)$  is constant over the relevant range of asymmetry energies. Nevertheless, our measurements do help to corroborate the assumptions made by Sethna for the scale of the asymmetry energy.

### B. Composition dependence of $\mathcal{P}$

We can make a more stringent test of the Sethna theory by looking for composition dependence in the density of tunneling states. We need to make one assumption in order to carry out this comparison: In the spirit of the model, we must assume that the parameter  $n(\delta)$ , whatever value it may have, is independent of concentration, or equivalently, that the maximum asymmetry energy  $\Delta_0$  is independent of concentration. Foote and Golding<sup>24</sup> show that  $\Delta_0$  is dependent on concentration for small  $x$  ( $x < 0.25$ ). For larger  $x$ , in the range in which we are working, our assumption may be more justified. The concentration dependence in the

$$\mathcal{P}(x, t = 1 \text{ sec})/\mathcal{P}(x = 0.7, t = 1 \text{ sec})$$

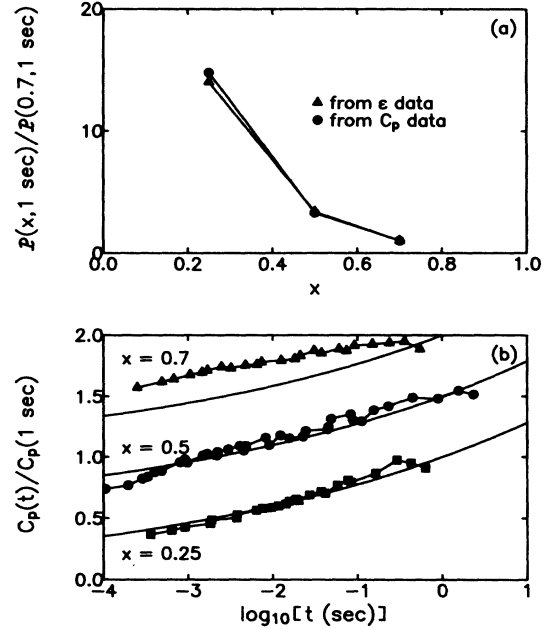


FIG. 7. (a) Normalized density of tunneling states as a function of CN concentration  $x$ . Values are from the present dielectric study and from the specific-heat data of Ref. 1. (b) Time-dependent specific heat of  $(\text{KBr})_{1-x}(\text{KCN})_x$  for three compositions. Values are normalized to unity at  $t = 1$  sec. The smooth curves are calculated from our dielectric measurements; the data are from Ref. 1. The vertical scale applies to  $x = 0.25$ ;  $x = 0.5$  and  $x = 0.7$  are offset for clarity.

calculation is thus determined only by the parameters of the distribution of barrier heights,  $\mathcal{P}(E)$ .

Table I and Fig. 7(a) show values for

$$\mathcal{P}(x, t = 1 \text{ sec})/\mathcal{P}(x = 0.7, t = 1 \text{ sec})$$

for  $x = 0.25, 0.5$ , and  $0.7$ , both calculated from our dielectric data and derived from specific-heat measurements. The agreement is remarkable, with a maximum difference of 6% between the derivations for the two different measurements. The distribution of barrier heights and, consequently, the density of tunneling levels, changes quite a bit from one concentration to the next. The  $\mathcal{P}(x, t = 1 \text{ sec})/\mathcal{P}(x = 0.7, t = 1 \text{ sec})$  values we calculate thus vary over more than an order of magnitude, with more tunneling levels for lower CN concentrations. The fact that the calculations follow the specific-heat data so closely over this entire range supports the tunneling level model of  $(\text{KBr})_{1-x}(\text{KCN})_x$ .

### C. Time dependence in $C_p$

The final independent variable we can vary to test the range of validity of the Sethna model is the measurement time  $t$ . We study the time dependence by normalizing calculated curves of  $C_p(t)$  to their values at  $t = 1$  sec. Our results are thus sensitive to only that part of the specific-heat calculation which determines the time

dependence, i.e., the distribution of barrier heights. Since each composition is normalized to its own  $t = 1$  sec value, and not to a common value, there are no free parameters or assumptions of composition independence of any quantity in this analysis. The time dependence in the calculated specific heat comes from the rate factor  $1 - \exp[-\Gamma(E)t]$ ,  $\Gamma(E)$  [see Eq. (1)] being the tunneling rate for a state with barrier energy  $E$ . This rate term weights the distribution of barrier energies,  $P(E)$ , so that high barrier states, which are slow to tunnel, contribute little to  $C_p$ . As we increase  $t$ , we include more high barrier states in the calculation. The number of states increases very slowly, approximately logarithmically with  $t$ , as can be seen from Eq. (1). The curves of  $C_p(t)/C_p(1 \text{ sec})$  we have calculated (Fig. 7) show little change with CN concentration. This is due to the fact that the tails of  $P(E)$  for all  $x$  studied are very similar. We have verified that any distribution of barrier energies sufficiently close to linear, as are the Gaussian tails, shows much the same time dependence. Note that the curves do not indicate logarithmic time dependence, as predicted by the standard two-level-system model, but rather curve away slowly from such behavior. Over the few decades of measurement time typical of specific-heat measurements, however, it is impossible to distinguish experimentally the difference between the predictions of the simple two-level model and those of our density-of-states calculations.

Comparison of our calculations with the time-dependent specific-heat measurements of De Yoreo *et al.*<sup>1</sup> shows excellent agreement over the 5 decades in  $t$  that the measurements cover. For both  $x = 0.25$  and  $0.5$  the calculated curves are well within the experimental error of the  $C_p$  data. The  $x = 0.7$  curve is also quite encouraging, showing essentially the same average slope as the data. The performance of Sethna's model is quite impressive. With no free parameters, and built from first-principles considerations, we see a prediction of time-dependent specific heat of a glassy system in quantitative agreement with experiment.

#### D. Phase-transition model and $\sigma(T)$

Since both  $E_0$  and  $T_g$  are proportional to the degree of quadrupolar ordering in  $(\text{KBr})_{1-x}(\text{KCN})_x$ , they should be proportional to one another. Listed in Table I are values of  $E_0/T_g$  for all three glassy compositions, and the values are indeed constant to within experimental uncertainty. This result supports the notion that the dielectric response of  $(\text{KBr})_{1-x}(\text{KCN})_x$  is a probe of the system's quadrupolar ordering.

We now focus on the temperature dependence of the barrier distribution widths,  $\sigma$ , plotted in Fig. 6. A linearly decreasing  $\sigma(T)$  suggests a similar trend in the average barrier energy  $E_0$ , which is consistent with the mean-field theory<sup>17</sup> of the quadrupolar freezing transition, since the theory holds that the quadrupolar order parameter decreases approximately linearly with  $T$  at low temperature. Dielectric measurements are sensitive to this order. This implies that  $E_0$  also decreases with temperature, and we understand the trends in  $\sigma(T)$  and  $E_0(T)$  according to

the schematic diagram shown in the inset of Fig. 6. Both  $\sigma$  and  $E_0$  tend to zero at the same temperature.

While it is true that the derivation of the convolution expression [Eq. (12)] requires activated behavior, normally the result of a constant activation energy, we can easily include a linear  $T$  dependence in  $E_0$ . We let

$$E'_0 = E_0 - \alpha T, \quad (20)$$

with  $\alpha$  a positive constant, which merely changes the measured Arrhenius prefactor  $\omega_0$ :

$$\begin{aligned} \omega_p &= \omega'_0 e^{-(E_0 - \alpha T)/k_B T} = \omega'_0 e^{\alpha/k_B} e^{-E_0/k_B T} \\ &= \omega_0 e^{-E_0/k_B T}. \end{aligned} \quad (21)$$

The substitution of  $E'_0$  for  $E_0$  does not in any way change the form of Eq. (17).  $E_0$  now has the meaning of the average barrier height at zero temperature. We can estimate  $\alpha$  by requiring Eqs. (19) and (20) to extrapolate to zero at the same temperature; thus  $\alpha = (E_0/\sigma_0)\beta$ , where  $\beta$  is simply the slope in Fig. 6. Values for  $\alpha$  are listed in Table I.

The addition of the  $\alpha$  term in Eq. (21) is particularly attractive in that not only does it help to tie together the phase-transition model and the convolution of barrier energies, but it explains the anomalously high attempt frequencies measured in  $(\text{KBr})_{1-x}(\text{KCN})_x$ . We identify  $\omega_0 = \omega'_0 e^{\alpha/k_B}$  as the measured attempt frequency, and obtain values for the true attempt frequency,  $\omega'_0$ . The values are shown in Table II and are more consistent with values commonly found in solids. We note that  $\omega'_0$  is more nearly independent of concentration than is  $\omega_0$ .

Also,  $\omega'_0$  is quite close to the value calculated for the frequency of oscillation,  $\omega_{\text{harm}}$ , of a CN rotor in a harmonic well approximating the actual potential. We have  $\omega_{\text{harm}} = (2E_0/I)^{1/2}$ , where  $E_0$  is the average barrier height and  $I$  is the effective moment of inertia of the CN molecule in the KBr lattice. Throughout our range of composition,  $\omega'_0$  is consistently within a factor of 2 of  $\omega_{\text{harm}}$ , giving further indication that  $\omega'_0$  is the true attempt frequency in  $(\text{KBr})_{1-x}(\text{KCN})_x$ .

A recent theory<sup>25</sup> has further connected the frequency of CN oscillation (librational modes) to the excess specific heat and to the plateau in plots of thermal conductivity,  $\Lambda$ , versus  $T$ . By adding this extra mechanism into calculations of the thermal properties, one obtains values for  $C_p$  and  $\Lambda$  in qualitative agreement with the data.<sup>1,2</sup> The

TABLE II. Attempt frequency values (in rad/sec) for  $(\text{KBr})_{1-x}(\text{KCN})_x$ .  $\omega_0$  is the apparent attempt frequency, obtained by fits to an activated form.  $\omega'_0$  is the corrected attempt frequency, given by  $\omega_0 = \omega'_0 e^{\alpha/k_B}$ .  $\omega_{\text{harm}}$  is the frequency of oscillation of a CN rotor in a harmonic potential, and  $\omega_{\text{lib}}$  is the CN libration frequency used in Ref. 25 to fit the data in Ref. 1.

$x$	0.25	0.5	0.7
$\omega_0$	$(8.2 \pm 2) \times 10^{13}$	$(2.8 \pm 1) \times 10^{14}$	$(5.7 \pm 1) \times 10^{14}$
$\omega'_0$	$(1.1 \pm 0.3) \times 10^{13}$	$(1.2 \pm 0.4) \times 10^{13}$	$(1.8 \pm 0.3) \times 10^{13}$
$\omega_{\text{harm}}$	$6.4 \times 10^{12}$	$8.3 \times 10^{12}$	$9.2 \times 10^{12}$
$\omega_{\text{lib}}$	$2.1 \times 10^{12}$	$3.5 \times 10^{12}$	

value of the libration frequency,  $\omega_{\text{lib}}$ , which best fits the thermal data is given in Table II. It is consistently lower than both  $\omega'_0$  and  $\omega_{\text{harm}}$ , but indicates at least a qualitative connection between  $\omega'_0$  and  $\omega_{\text{lib}}$ .

### E. $\mathcal{P}$ versus $1/T_q$

The scope of this experiment gives us the opportunity to consider the relation between the low-temperature density of tunneling states  $\mathcal{P}$  and the glass-transition temperature  $T_g$ . The traditional two-level-system model approach is to assume a flat distribution of asymmetry energies. Since the glass-transition temperature sets a natural energy cutoff for the distribution, the integrated density of states is then inversely proportional to  $T_g$ . This result has been derived in a more rigorous manner using a free-volume description of the glass transition.<sup>26</sup> Experimental evidence for the relation has been ambiguous at best.<sup>27</sup>

In  $(\text{KBr})_{1-x}(\text{KCN})_x$  we can evaluate  $\mathcal{P}$  as a function of the transition temperature since we know the distributions of tunneling-level energies for compositions with different values of  $T_g$ . To do this we Taylor-expand the Gaussian  $P(E)$  about  $E=0$ , keeping only terms up to order  $E^2$ , and substitute into Eq. (2):

$$\mathcal{P} = \frac{n(\delta)}{A} \frac{x E_{\text{max}}}{\sqrt{\pi} \sigma_0} \exp[-(E_0/\sigma_0)^2] \times \left[ 1 + \left[ \frac{E_0}{\sigma_0^2} \right] E_{\text{max}} + \left[ \frac{2E_0^2 - \sigma_0^2}{3\sigma_0^4} \right] E_{\text{max}}^2 + \dots \right], \quad (22)$$

where we have approximated the rate term in Eq. (2) by a step function with turnover at  $E = E_{\text{max}}(t)$ . There are three independent energy scales that appear in this equation.  $\Delta_0$  sets the scale for the splitting of the tunneling levels,  $E_0$  sets the energy scale for the barrier heights, and  $\sigma_0$  sets the scale for the energy width of the distribution. We have already argued that  $\Delta_0$  depends on the dipolar and not on the quadrupolar interactions and is therefore independent of  $T_q$ . The mean-field theory tells us that  $E_0$  and  $T_q$  are both proportional to the quadrupolar interaction strength, so we can assume that

$$E_0 = c_E T_q. \quad (23)$$

Indeed, values of  $E_0/T_q$  (Table I) are approximately constant. The CN concentration  $x$  determines the number of nearest neighbors and therefore the interaction strength. It too should be proportional to  $T_q$ ,

$$x = c_x T_q. \quad (24)$$

Various experimental probes support this claim.<sup>3-9</sup> The connection between  $\sigma_0$  and  $T_q$ , however, is far less clear. Figure 5 shows  $\sigma_0$  as weakly dependent on  $x$  (and thus on  $T_q$ ), with no obvious functional form for  $\sigma_0(T_q)$ . Substituting Eqs. (23) and (24) into Eq. (22), we find

$$\mathcal{P} = \frac{n(\delta)}{A} \frac{c_x E_{\text{max}}}{\sqrt{\pi} \sigma_0} \exp[-(c_E T_q/\sigma_0)^2] \times \left[ \left[ 1 - \frac{E_{\text{max}}^2}{3\sigma_0^2} \right] T_q + \left[ \frac{c_E}{\sigma_0^2} E_{\text{max}} \right] T_q^2 + \left[ \frac{2c_E^2}{3\sigma_0^4} E_{\text{max}}^2 \right] T_q^3 + \dots \right]. \quad (25)$$

This expression does not have a particularly simple form such as has been suggested in the past. This is because there is more than one important energy scale. Although  $E_0$  does scale with  $T_q$ ,  $\sigma_0$  and  $\Delta_0$  do not. In the particular case of  $(\text{KBr})_{1-x}(\text{KCN})_x$ , we have calculated the complete dependence of  $\mathcal{P}$  on  $T_q$  and find that as  $T_q$  increases  $\mathcal{P}$  decreases.

From this analysis we would like to see how  $\mathcal{P}$  and  $T_g$  may be related, in general, for all glasses. Even though we believe that the general method proposed here for calculating  $\mathcal{P}$  in this glassy crystal may be applicable to glasses in general, the fact that there are three different energy scales (instead of only one, as has been tacitly assumed) immediately indicates that there should be no simple relation between  $\mathcal{P}$  and  $T_g$ . However, we might find some correlations when we are dealing with a particular class of glass-formers when we know, for example, that we are only varying one of these energies at a time. In particular, for the case that  $\sigma_0$  is proportional to  $T_g$  and  $\Delta_0$  is constant, there is only one energy scale in the problem and we can argue that  $\mathcal{P} \sim 1/T_g$ .

### F. Other glassy systems

It is not clear at present how the microscopic model of  $(\text{KBr})_{1-x}(\text{KCN})_x$  can be generalized to other glassy materials. Indeed, some recent work may indicate that the picture of flipping molecules as the dominant glassy dynamical process cannot be applied in a straightforward manner to a related orientational glass system.<sup>28</sup> We believe, however, that the wealth of data on  $(\text{KBr})_{1-x}(\text{KCN})_x$  indicates that we can understand the glassy behavior of this system using a simple and intuitively appealing model. This model presents a coherent picture of low-temperature thermal properties, intermediate-temperature  $\beta$  relaxation, and a high-temperature glasslike transition, all within a common framework based on the flipping of cyanide molecules. At low temperatures, the picture is close to that of the tunneling-level model already widely used in the realm of real glasses. The challenge remains to cast the  $(\text{KBr})_{1-x}(\text{KCN})_x$  model into a form which can embrace the apparent variety of real-glass systems. It is now an experimental question whether one can relate the low-temperature thermal properties of glasses to the  $\beta$  relaxation that is often observed at higher temperatures. It is also an open question whether this  $\beta$  relaxation can be related to the order parameter of the glass transition, as we have shown to occur in  $(\text{KBr})_{1-x}(\text{KCN})_x$ . Clearly, further studies of  $\beta$  relaxation in structural glasses are warranted.

## ACKNOWLEDGMENTS

We thank N. O. Birge, Y. H. Jeong, J. P. Sethna, M. Meissner, and P. K. Dixon for stimulating discussions.

We are grateful to B. Golding and M. Foote for providing the  $x = 0.7$  sample. This work was supported by the U.S. National Science Foundation—Materials Research Laboratory under Grant No. DMR-85-19460.

- 
- <sup>1</sup>J. J. De Yoreo, W. Knaak, M. Meissner, and R. O. Pohl, *Phys. Rev. B* **34**, 8828 (1986); J. J. De Yoreo, M. Meissner, R. O. Pohl, J. M. Rowe, J. J. Rush, and S. Susman, *Phys. Rev. Lett.* **51**, 1050 (1983).
- <sup>2</sup>D. Moy, J. N. Dobbs, and A. C. Anderson, *Phys. Rev. B* **29**, 2160 (1984).
- <sup>3</sup>A. Loidl, R. Feile, and K. Knorr, *Phys. Rev. Lett.* **48**, 1263 (1982).
- <sup>4</sup>J. M. Rowe, J. J. Rush, D. G. Hinks, and S. Susman, *Phys. Rev. Lett.* **43**, 1158 (1979).
- <sup>5</sup>A. Loidl, K. Knorr, R. Feile, and J. K. Kjems, *Phys. Rev. Lett.* **51**, 1054 (1983); A. Loidl, R. Feile, K. Knorr, and J. K. Kjems, *Phys. Rev. B* **29**, 6052 (1984).
- <sup>6</sup>S. K. Satija and C. H. Wang, *Solid State Commun.* **28**, 617 (1978).
- <sup>7</sup>K. Knorr and L. Loidl, *Phys. Rev. B* **31**, 5387 (1985).
- <sup>8</sup>C. W. Garland, J. Z. Kwiecien, and J. C. Damien, *Phys. Rev. B* **25**, 5818 (1982); J. Z. Kwiecien, R. C. Leung, and C. W. Garland, *ibid.* **23**, 4419 (1981).
- <sup>9</sup>K. Knorr and A. Loidl, *Z. Phys. B* **46**, 219 (1982).
- <sup>10</sup>K. Knorr, U. G. Volkmann, and A. Loidl, *Phys. Rev. Lett.* **57**, 2544 (1986).
- <sup>11</sup>S. Bhattacharya, S. R. Nagel, L. Fleishman, and S. Susman, *Phys. Rev. Lett.* **48**, 1267 (1982); N. O. Birge, Y. H. Jeong, S. R. Nagel, S. Bhattacharya, and S. Susman, *Phys. Rev. B* **30**, 2306 (1984).
- <sup>12</sup>F. Lüty, in *Proceedings of the International Conference on Defects in Insulating Crystals*, edited by V. M. Turkevich and K. K. Swartz (Springer-Verlag, Berlin, 1981), p. 69; F. Lüty and J. Ortiz-Lopez, *Phys. Rev. Lett.* **50**, 1289 (1983).
- <sup>13</sup>G. P. Johari and M. Goldstein, *J. Phys. Chem.* **74**, 2034 (1970); **53**, 2372 (1970).
- <sup>14</sup>P. W. Anderson, B. I. Halperin, and C. M. Varma, *Philos. Mag.* **25**, 1 (1972).
- <sup>15</sup>W. A. Phillips, *J. Low Temp. Phys.* **7**, 351 (1972).
- <sup>16</sup>J. P. Sethna and K. S. Chow, *Phase Transitions* **5**, 317 (1985); M. Meissner, W. Knaak, J. P. Sethna, K. S. Chow, J. J. De Yoreo, and R. O. Pohl, *Phys. Rev. B* **32**, 6091 (1985); J. P. Sethna, *N.Y. Acad. Sci.* **484**, 130 (1986).
- <sup>17</sup>J. P. Sethna, S. R. Nagel, and T. V. Ramakrishnan, *Phys. Rev. Lett.* **53**, 2489 (1984).
- <sup>18</sup>L. Wu, R. M. Ernst, Y. H. Jeong, S. R. Nagel, and S. Susman, *Phys. Rev. B* **37**, 10444 (1988).
- <sup>19</sup>N. O. Birge and S. R. Nagel, *Rev. Sci. Instrum.* **58**, 1464 (1987).
- <sup>20</sup>K. S. Cole and R. H. Cole, *J. Chem. Phys.* **9**, 341 (1941).
- <sup>21</sup>G. Williams and D. C. Watts, *Trans. Faraday Soc.* **66**, 80 (1970).
- <sup>22</sup>E. C. Ziemath and M. A. Aegerter, *Solid State Commun.* **58**, 519 (1986).
- <sup>23</sup>D. W. Davidson and R. H. Cole, *J. Chem. Phys.* **19**, 1484 (1951).
- <sup>24</sup>M. C. Foote and B. Golding (unpublished).
- <sup>25</sup>M. Randeria and J. P. Sethna (unpublished); E. R. Grannan, M. Randeria, and J. P. Sethna, *Phys. Rev. Lett.* **60**, 1402 (1988).
- <sup>26</sup>M. H. Cohen and G. S. Grest, *Solid State Commun.* **39**, 143 (1981).
- <sup>27</sup>J. F. Berret and M. Meissner, *Z. Phys. B* **69**, 35 (1987).
- <sup>28</sup>C. I. Nicholls, L. N. Yadon, D. G. Haase, and M. S. Conradi, *Phys. Rev. Lett.* **59**, 1317 (1987).